Borehole stability in geothermal reservoirs – A combined laboratory and numerical approach

Justin Mattheis
Chair of Engineering Geology, Technical University of Munich, Munich, Germany

Catharina Drexl
Chair of Engineering Geology, Technical University of Munich, Munich, Germany

Martin Potten
Chair of Engineering Geology, Technical University of Munich, Munich, Germany

Georg Stockinger
Chair of Engineering Geology, Technical University of Munich, Munich, Germany

Kurosch Thuro
Chair of Engineering Geology, Technical University of Munich, Munich, Germany

ABSTRACT: Despite the well-known geothermal potential in the North Alpine Foreland Basin, large scale exploration is still limited by the economic risk of well instabilities originating from inadequate prediction of the heterogeneous rock mass conditions in the reservoir. One decisive factor is the rocks toughness against fracture propagation. Hence, analogs to the reservoir rocks are subject to Semi-circular Bend tests to determine the required energy for tensile fractures (mode I) and accordingly Double-edge Notched Brazilian Disk tests for shear fractures (mode II). The subsequent finite-discrete numerical simulations, in which the experimental results are implemented, show varying fracture patterns in the rock mass caused by drilling. The fracturing depends on the rock type, the pre-existing discontinuities, and the stresses in up to 5 km depth. Further expansion of this investigation to other scenarios and rock types, paired with a reliable geological prediction, reduces the associated risks for deep geothermal projects.

Keywords: geothermal reservoir characterization, borehole stability, fracture energy, laboratory tests, numerical FDEM modeling; North Alpine Foreland Basin (SE Germany).

1 INTRODUCTION

In the metropolitan area of Munich, the well-known hydrothermal reservoir in the North Alpine Foreland Basin (NAFB) provides a suitable renewable source for domestically and industrially demanded heat (Agemar et al. 2014). However, the heterogeneity of the reservoir is widely known and causes different hydraulic and mechanical properties of the rock mass. Increasing the understanding of subsurface processes is therefore a crucial task to significantly expand the share of geothermal heat supply in the heating sector. Besides the acting stress conditions, the geomechanical behavior of these deep wells is highly dependent on mechanical rock mechanical properties like strength, elastic behavior, and internal friction parameters. Furthermore, the pre-existing joints and faults in the rock mass, henceforth referred to as “discrete fracture network” (DFN), influence the rock mass behavior significantly with their roughness and their frictional and cohesive properties (Stockinger 2022; Zoback 2010).

2 STUDY AREA: THE UPPER JURASSIC RESERVOIR IN THE NAFB

The Upper Jurassic sedimentary rocks are considered an important aquifer due to their permeable, fluid-bearing, and deep rocks, within the NAFB in the south of Germany. They consist of predominantly marine limestones, marls, and dolomites. Based on different characteristics, the Upper Jurassic carbonates are usually divided into a massive reef facies and a stratified basin facies (Meyer & Schmidt-Kaler 1989). After deposition of the Mesozoic sediments, the complicated tectonic processes of the Alpine orogenesis formed a trough filled with debris from the Alps and the Bohemian Massif (Lemcke 1973). Due to the southwards increasing overburden of Tertiary sediments, the Upper Jurassic Carbonates now dip from north to south towards the Alps and can be found at depths of up to 4,500 m (Agemar et al. 2014). At this depth, the geothermal gradient causes rock and fluid temperatures of up to 140 °C (Agemar et al. 2014).

Studies on carbonates in the reservoir have already been conducted to describe and explore their heterogeneous structures. However, these investigations are mostly limited to microscopic-scale methods, as drill core material from the reservoir from depths of up to 4,500 m is extremely limited. Based on this and on the Upper Jurassic Carbonates surface outcrops north of the NAFB, analog studies have proven to be an effective means of determining rock properties. Analog rocks from quarries with similar stratigraphy, lithology, and age as to those in the reservoir are easier to obtain in larger quantities and thus also suitable for specimen preparation for destructive laboratory testing.

Some geomechanical studies on analog rocks of the Upper Jurassic reservoir focusing on porosity properties, elasticity and strength parameters have already been performed (Hedtmann & Alber 2017; Mraz et al. 2018). However, there is currently no experimental data for both the fracture toughness in tension (Mode I) and in shear (Mode II) for the reservoir rocks or rocks analogous to them. Nonetheless, these characteristic values are indispensable for realistic and meaningful numerical modeling using the FDEM approach (Geomechanica 2016).

Based on the geomechanical characterization of analog rocks by Mraz et al. (2018) and Stockinger (2022), the following analog rocks from the Swabian and Franconian Alb were chosen for laboratory investigations: “Bankkalk”, “Dietfurter Kalkstein”, and “Pfraundorfer Dolomit”. These three rocks represent a first approximation of the geologically heterogeneous properties of the reservoir. All three rocks have already been adequately characterized in terms of their lithological and rock mechanical properties (Mraz et al. 2018; Stockinger 2022). Also, data on the mode II fracture energy of the Pfraundorfer Dolomit has recently been published by our group (Hug et al. 2022).

3 LABORATORY EXPERIMENTS

To determine the fracture toughness, the experimental setup of the Semi-circular Bend (SCB) test according to Kuruppu et al. (2014) and the setup of the Double-edge Notched Brazilian Disk (DNBD) test according to Bahrami et al. (2020) were used (Fig. 1). Both the test setups and the calculation of fracture toughness were carried out according to the specifications of the respective publications. For both types of tests, hardwood strips were placed between the specimen and the test fixture to achieve better contact of the specimen surface to the load application.

In the context of linear elastic fracture mechanics, the fracture energy G_C was calculated analogous to Hug et al. (2022) from the fracture toughness K_C and Young’s modulus E using the following equation:

$$G_{C\,I/II} = \frac{(K_{C\,I/II})^2}{E} \tag{1}$$

For the calculation of the fracture energy, the already determined, rock-specific parameters of the Young's modulus of Stockinger (2022) were adopted. Due to material limitations the SCB-tests on the “Dietfurter Kalkstein” samples were performed on smaller disks than recommended by Kuruppu et al. (2014). The resulting fracture toughness and fracture energy values are shown in Tab. 1 with their respective statistical distribution. The median fracture energy values are used for further analysis.

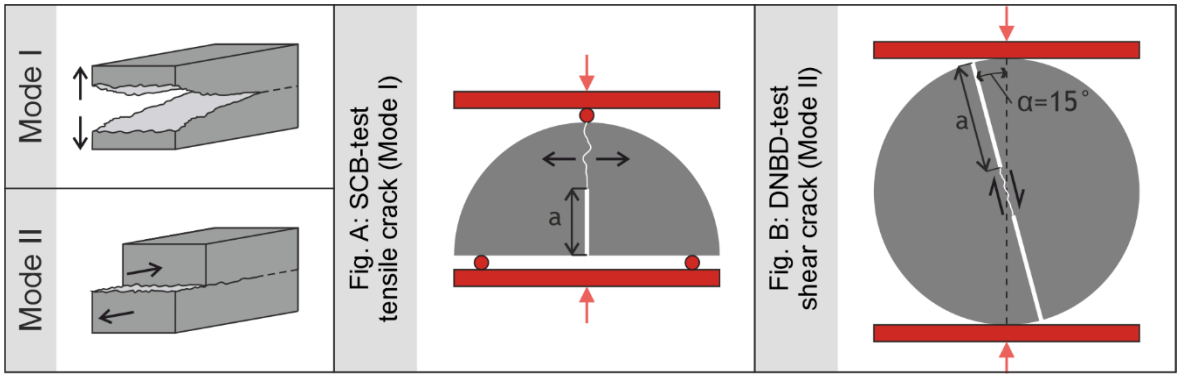

Figure 1. Illustration of the fracture modes and test setup for the SCB test according to Kuruppu et al. (2014) and DNBD test according to Bahrami et al. (2020).

Table 1. Parameters for the determination of the fracture energy Mode I and Mode II.

Parameter		Bankkalk		Dietfurter Kalkstein		Pfraundorfer Dolomit	
Young's modulus *[GPa]*[2]		23.7[1]		39.5[1]		52.3[1]	
		Fracture Toughness *[MPa√m]*	Fracture Energy *[N/m]*	Fracture Toughness *[MPa√m]*	Fracture Energy *[N/m]*	Fracture Toughness *[MPa√m]*	Fracture Energy *[N/m]*
Mode I	Mean	n. m.	n. m.	1.39	52.5	1.11	24.0
	Median	**n. m.**	**n. m.**	**1.38**	**48.5**	**1.10**	**23.2**
	Stdv	n. m.	n. m.	0.37	26.0	0.12	5.0
	number	-		*3*		*24*	
Mode II	Mean	1.79	137.4	3.03	235.0	4.45[2]	394.4[2]
	Median	**1.78**	**133.0**	**3.10**	**243.9**	**4.63[2]**	**409.3[2]**
	Stdv	0.20	31.1	0.30	45.3	0.92[2]	149.5[2]
	number	*8*		*6*		*18*	

n. m. = not measured; [1] after Stockinger (2022); [2] after Hug et al. (2022)

4 FINITE-DISCRETE NUMERICAL MODEL OF THE BOREHOLE VICINITY

4.1 Methods

To apply the insights from the centimeter-scale laboratory tests to the dimensions of a borehole, a numerical model is chosen that shows the rock mass's response to the excavation process. Production and reinjection of thermal water and hydraulic stimulation will be discussed in future works.

The FDEM (finite-discrete element method) simulation is performed with the software Irazu by Geomechanica. As shown in Fig. 2 d), the rock mass is represented by triangular elastic mesh elements. Between them, rectangular crack elements are implemented to control the initiation and propagation of fractures in the previously intact rock. If a certain threshold stress is exceeded, a fracture forms and yields until further stress causes the mesh elements to break fully apart (Fig. 2 a–c). Around the new fracture, the finite stress-strain calculation now continues as discrete calculation (Mahabadi et al. 2012; Geomechanica 2016).

The modeled scenarios consist of horizontal 2D planes intersecting the vertical borehole at depths of 1, 3 and 5 km. The model area is set up by a 12 m x 12 m square with a 15 cm wide circular borehole in the center. To reduce computing time, the borehole mesh refines in rectangles around the borehole. This refinement leads from a mesh size of 0.7 m at the outer boundary to a factor of 0.02 m at the borehole. The boundary condition allows no displacements of the outer boundary nodes. Three different materials are investigated that represent the reservoir rocks to a large extent (Tab. 2).

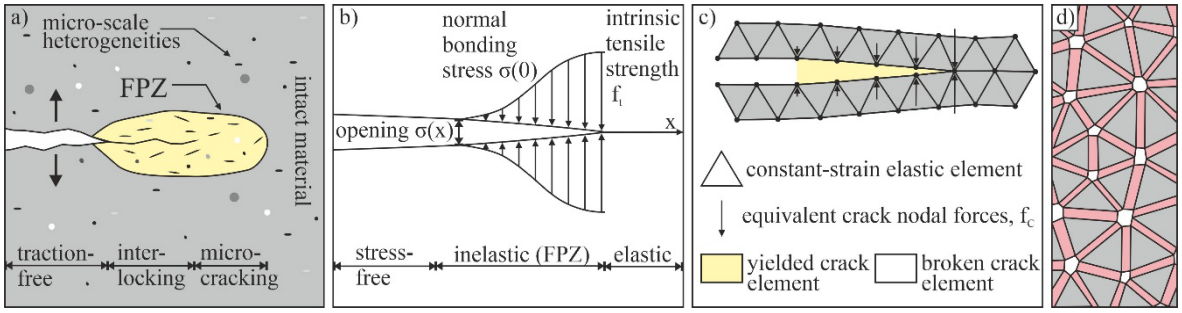

Figure 2. Mathematical implementation of the combined finite-discrete element method in a 2D numerical model, modified after Lisjak et al. (2013).

The density, static Young's modulus, tensile strength, and Poisson's ratio were determined by Potten (2020) on numerous in-situ reservoir samples. These diverse samples are regrouped into the homogenous groups "limestone", "strong limestone" and "dolostone". It is noted that the terminology differs from the categories assigned by Stockinger (2022), because deviating classification criteria were used. Suitable analog rocks are assigned to these groups to allow for fracture energies testing despite limited in-situ material. Namely the "Bankkalk" represents the (weaker) limestone, the "Dietfurter Kalkstein" represents the strong limestone and the "Pfraundorfer Dolomit" the dolostone-category.

The cohesion and, for the limestone, the fracture Energy I are estimated based on existing strength parameters by Irazu. The coefficient of friction is kept constant at 0.6 through all lithologies. Based on the investigations of Potten (2020) the in-situ stress state is assumed to be exactly between a normal faulting and strike slip regime, with the effective stresses defined as:

$$\sigma_v = \sigma_{Hmax} = 13.2\ MPa/km\ ;\ \sigma_{hmin} = 4.19\ MPa/km \qquad (2)\ (3)$$

Table 2. Experimentally determined material input parameters used in the numerical models.

Material	Density ρ_b [g/m³]	Young's modulus E [GPa]	Poisson's ratio ν [-]	Tensile strength σ_t [MPa]	Cohesion c [MPa]	Fracture Energy I G_{CI} [N/m]	Fracture Energy II G_{CII} [N/m]
Limestone	2.61[2]	43.0[2]	0.15[2]	5.6[2]	18.0[2]	13.3[1]	133.0
Strong Limestone	2.63[2]	49.4[2]	0.14[2]	10.1[2]	31.0[2]	48.5	243.9
Dolostone	2.67[2]	53.0[2]	0.09[2]	10.1[2]	20.0[2]	23.2	409.3[3]

[1] estimated by Irazu; [2] after Potten (2020); [3] after Hug et al. (2022)

Three discrete fracture networks (DFNs) are defined with the parameters shown in Tab. 3. These parameters, the penalty values and the orientation and persistence of the DFN are taken from the values assigned by Stockinger (2022) to his models of the geothermal wells in Geretsried in the central NAFB. All other input parameters for the models are kept at default.

Table 3. DFN input parameters used in the numerical models after Stockinger 2022.

Discrete fracture network	Tensile strength σ_t [MPa]	Cohesion c [MPa]	Fracture Energy I G_{CI} [N/m]	Fracture Energy II G_{CII} [N/m]	Coefficient of friction μ [-]
DFN 1	broken	broken	broken	broken	0.3
DFN 2	0.1	0.5	1	5	0.4
DFN 3	0.1	0.5	1	5	0.4

4.2 Results

The total number of 500,000 timesteps was not reached in every model due to numerical instabilities that occurred after complete disintegration of the rock near the borehole. For comparability, all models are analyzed after 235,000 timesteps, which is after the finished excavation of the borehole (at 200,000 steps), but before stable equilibrium is reached in all cases. Nevertheless, all models show already at this timestep clear indications whether the wellbore integrity is threatened or not. At 1 km depth, the rock mass is barely influenced by the excavation. Except for small wing cracks at the tip of DFN 2 and 3, especially in the limestone, no destabilizing effects are noticed. At 3 km depth, shear and tensile fractures surround the borehole and occur in areas where the DFN are minimally spaced. For the strong limestone and dolostone the borehole can be considered stable. While the total number of fractures and the disintegration of larger areas increase further at 5 km depth, the orientation and location of the fractures show a comparable trend.

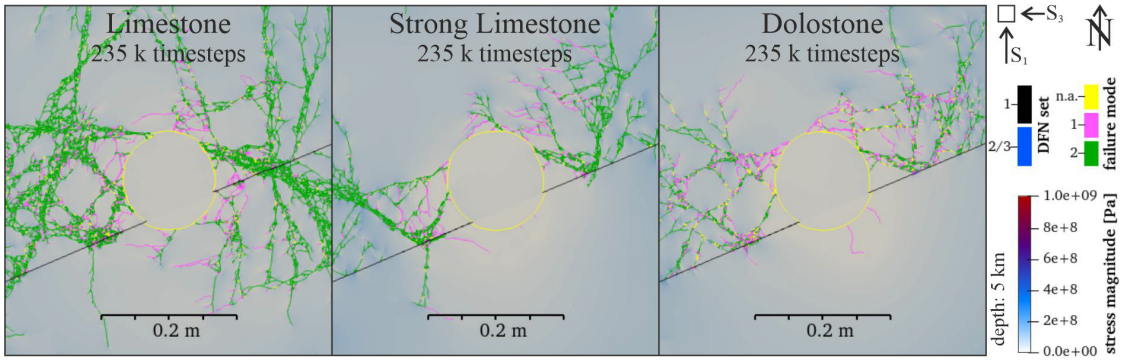

Figure 3. Resulting fracture patterns shortly after borehole excavation in different lithologies.

Wedge-shaped borehole breakouts occur in all models deeper than 1 km. Their orientation is roughly in S_3/S_{hmin} (E-W) direction, but mostly controlled by the orientation of the continuous DFN 1 (Fig. 3). As shown in Stockinger (2022), different DFN orientations could result in misleading orientation of borehole breakouts that are DFN-controlled and not always parallel to S_3/S_{hmin}, as in this case. The resulting wedges are pushed into the excavated area and steadily lower the effective well radius. At the tips of the wedge, the developing voids are the cause for a strongly disintegrated rock mass, which in some cases provides stress peaks that prematurely end the calculation process. As shown in Fig. 4, the total number of created fractures increases with depth for all rock types over several orders of magnitudes up to a maximum of about 50,000 fractured mesh elements (limestone). Regardless of the lithology, mode II fractures are not relevant at 1 km depth. Two kilometers deeper, however, shear fractures are by a large margin more abundant than mode I fractures. As in 5 km depth, they control the total fracture extent. At all depths, the number of fractured elements for the strong limestone and dolostone is comparable, yet significantly lower than for the weaker limestone.

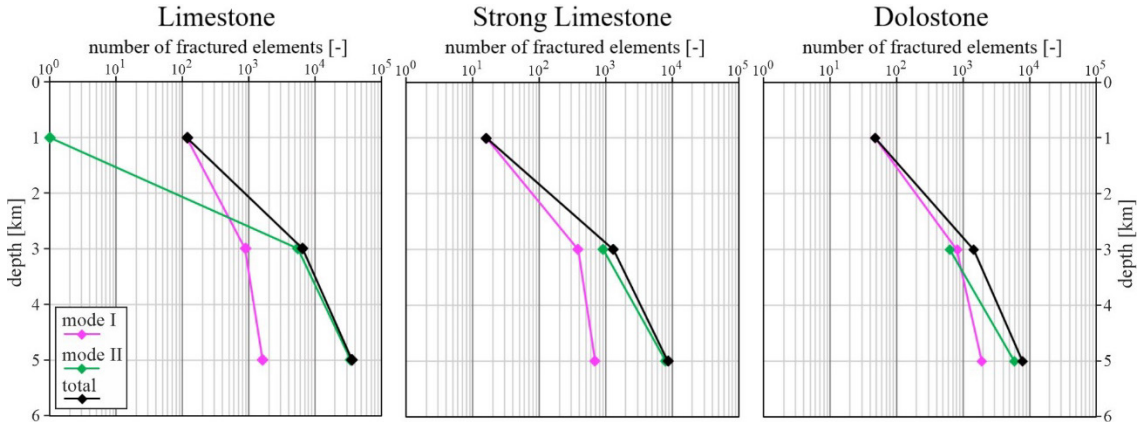

Figure 4. Total number of fractured elements in the modelled area of different lithologies and depths.

5 CONCLUSION

This work shows the importance of laboratory testing analog samples for characterizing a geothermal reservoir and not to rely on in-situ cores only. The results presented here suggest that, despite the partly substantial standard deviation of results, it is recommended to determine the fracture energies experimentally as they vary depending on the rock type. Additionally, fracture energies are one of the most important input parameters controlling the model's stability. The numerical models show potentially problematic scenarios regarding wellbore integrity and show that depth and thus the corresponding in-situ stresses, lithologies but also the DFNs that limit the fracture propagation in many places, contribute. Also, in all models deeper than 1 km, it is consistent that mode II fractures control the total degree of fracturing. In these models, mode I fractures occur only secondarily between existing shear fractures, yet without impacting the overall stability. Apart from the total sum of fractured elements, further indicators of borehole stability will be included in future work. Expanding the models to more diverse scenarios and including more experimentally determined laboratory data will cover increasingly more scenarios that are encountered in reality and lead to a more predictable overall estimate of wellbore integrity.

Acknowledgements: This work is part of the Geothermal-Alliance Bavaria and funded by the Bavarian State Ministry of Science and Arts (StMWK). The authors appreciate the assistance of Dr. Heiko Käsling in establishing an experimental setup for the SCB-tests. We also thank Ridvan Yildirim, who performed parts of the data analysis and modeling work as part of his master thesis.

REFERENCES

Agemar, T., Weber, J. & Schulz, R. (2014). Deep Geothermal Energy Production in Germany. *Energies*, *7*(7), 4397–4416.

Bahrami, B., Nejati, M., Ayatollahi, M., Driesner, T. & Bahramit, B. (2020). Theory and experiment on true mode II fracturing of rocks. *Engineering Fracture Mechanics*, *240*(1).

Geomechanica. (2016). *Irazu FDEM Theory Manual.*

Hedtmann, N. & Alber, M. (2017). Investigation of Water-permeability and Ultrasonic Wave Velocities of German Malm Aquifer Rocks for Hydro-Geothermal Energy. *Procedia Engineering*, *191*, 127–133.

Hug, L., Potten, M., Stockinger, G., Thuro, K. & Kollmannsberger, S. (2022). A three-field phase-field model for mixed-mode fracture in rock based on experimental determination of the mode II fracture toughness. *Engineering with Computers*.

Kuruppu, M.D., Obara, Y., Ayatollahi, M.R., Chong, K.P. & Funatsu, T. (2014). ISRM-Suggested Method for Determining the Mode I Static Fracture Toughness Using Semi-Circular Bend Specimen. *Rock Mechanics and Rock Engineering*, *47*(1), 267–274.

Lemcke, K. (1973). Zur nachpermischen Geschichte des nördlichen Alpenvorlandes. In Bayer. Geologisches Landesamt (Ed.), *Geologica Bavarica* (Vol. 69). Bayer. Geologisches Landesamt.

Lisjak, A., Liu, Q., Zhao, Q., Mahabadi, O.K. & Grasselli, G. (2013): Numerical simulation of acoustic emission in brittle rocks by two-dimensional finite-discrete element analysis. - Geophys. J. Int. 195: 423–443, Oxford (Oxford University Press).

Mahabadi, O.K., Lisjak A, Munjiza A, Grasselli G (2012). Y-Geo: new combined finite-discrete element numerical code for geomechanical applications. Int J Geomech 12(6):676–688.

Meyer, R.K.F. & Schmidt-Kaler, H. (1989). Paläogeographischer Atlas des süddeutschen Oberjura (Malm). *Geologisches Jahrbuch*, *A 115*, 1–77.

Mraz, E. (2019). *Reservoir Characterization to Improve Exploration Concepts of the Upper Jurassic in the Southern Bavarian Molasse Basin* [Ph.D.-thesis]. Technical University of Munich, Munich.

Mraz, E., Bohnsack, D., Stockinger, G., Käsling, H. & Thuro, K. (2018). Die Bedeutung von Analogaufschlüssen des Oberjura für die Interpretation der Lithologie der geothermalen Tiefbohrung Geretsried. *Jahresberichte Und Mitteilungen Des Oberrheinischen Geologischen Vereins*, *100*, 517–548.

Potten, M. (2020). *Geomechanical characterization of sedimentary and crystalline geothermal reservoirs* [Ph.D.-thesis]. Technical University of Munich, Munich.

Stockinger, G. (2022). *Fracturing in Deep Boreholes* [Ph.D.-thesis]. Technical University of Munich, Munich.

Zoback, M. D. (2010): Reservoir geomechanics. – 2nd ed., 449 p., Cambridge (Cambridge University Press).